Charge excitations in NaV_2O_5

A. Hübsch, C. Waidacher, and K. W. Becker Institut für Theoretische Physik, Technische Universität Dresden, D-01062 Dresden, Germany

W. von der Linden

Institut für Theoretische Physik, Technische Universität Graz, Petersgasse 16, A-8010 Graz, Austria (November 1, 2018)

We calculate the electron-energy loss spectrum and the optical conductivity for NaV_2O_5 using the standard Lanczos algorithm. The vanadium ions in NaV_2O_5 form a system of coupled ladders which can be described by a quarter-filled extended Hubbard model. Since this system has a large unit cell, one has to be very careful to avoid finite-size effects in the calculations. We show this by performing exact diagonalization of different clusters with up to 16 sites. The calculated loss function for the extended Hubbard model shows good agreement with experimental spectra. Furthermore, a qualitative description of the optical conductivity is obtained with the same Hamiltonian, and the same set of model parameters. The comparison with the experiment shows that interladder hopping is of minor importance for a realistic description of charge excitations in NaV_2O_5 . We find that the character of the excitations depends strongly on the direction of momentum transfer.

PACS numbers: 71.27.+a, 71.45.Gm, 71.10.Fd

I. INTRODUCTION

The insulating system α' -NaV₂O₅ belongs to the fascinating class of highly correlated low-dimensional electronic systems. Recently, its physical properties have been intensively investigated theoretically as well as experimentally. The magnetic susceptibility of NaV₂O₅, can be well described by a S = 1/2 antiferromagnetic Heisenberg chain with exchange interactions of J = 440 Kand 560K for temperatures below and above the transition temperature $T_C \approx 34$ K. The opening of a spin gap at the phase transition is accompanied by unit cell doubling in the a and b direction, and quadrupling in the cdirection.³ Based on an early X-ray study⁴ which postulated two different V sites, i.e. magnetic V⁴⁺ chains along the b axis separated by non-magnetic V^{5+} chains, α' -NaV₂O₅ was initially identified as an inorganic spin-Peierls (SP) material² similar to CuGeO₃. However, according to a recent crystal structure analysis,⁵ at room temperature all V sites are equivalent with a formal valence +4.5. Therefore, the V sites form a quarter-filled ladder⁶ which can be mapped onto a S = 1/2 chain,⁷ and the resulting exchange couplings J along the chain agree well with the experimental data. In principle, this effective chain may show all features of an ordinary onedimensional S = 1/2 Heisenberg chain, including the spin-Peierls transition. On the other hand, various experimental results for NaV₂O₅ indicate a more complicated transition at T_C : The BCS ratio of $2\Delta/kT_C$ for the dimerization gap Δ at zero temperature has the anomalously high value of 6.44. The phase transition consists of two very close transitions,⁸ and two inequivalent V sites were detected by NMR,⁹ and attributed to V⁴⁺ and V⁵⁺. This has motivated both theoretical and experimental work, proposing a pure charge ordering (CO) instability^{10,11} or CO coupled to SP distortion.^{12,13} Recently, the space group Fmm2 for the low-temperature crystal structure was determined from x-ray scattering data, ¹⁴ and three inequivalent V sites in the V⁴⁺, V⁵⁺, and V^{4.5+} oxidation states were proposed. ^{15,16} Since this space group is incompatible with the NMR measurement the low-temperature crystal structure and the charge ordering pattern are still under discussion. ^{17,18}

Charge ordering can be viewed as a Wigner-crystallization on a lattice, 19 which is caused by long-range Coulomb interaction. Thus different models with nearest-neighbor Coulomb repulsions were studied 10,20,21 and an in-line 12 and a zig-zag structure 10,11 for $\rm NaV_2O_5$ were proposed. The calculation of excitation spectra is a powerful test for these models, as they can be directly compared with experimental data.

Recently, we studied 22 the dynamic dielectric response of NaV₂O₅ using an effective quarter-filled ladder model (see Sec. II). In the present paper we improve on these calculations by treating the complete extended Hubbard model. Furthermore, we study the role of the interladder hopping in more detail. We analyze possible finite-size effects in cluster calculations for NaV₂O₅, and in particular, we discuss the optical conductivity. While in previous work 23,24 different models were used for the calculation of the optical conductivity and the dynamical density correlation function, we describe both with the same Hamiltonian, and the same set of model parameters.

The paper is organized as follows. In Sec. II, general aspects of our approach are presented. The value of the interladder hopping is discussed in Sec. III. Finite-size effects of cluster calculations are investigated in Sec. IV. Section V contains the comparison of our results of the dynamic dielectric response with experimental spectra of $\rm NaV_2O_5$, and in Sec. VI we discuss the optical conductivity. Finally, the conclusions are presented in Sec. VII.

II. GENERAL ASPECTS OF THE CALCULATIONS

We study the dynamic dielectric response and the optical conductivity assuming that the electrons in NaV₂O₅ can be described by a quarter-filled extended Hubbard

$$\mathcal{H} = -\sum_{\langle i,j\rangle,\sigma} t_{ij} \left(c_{i,\sigma}^{\dagger} c_{j,\sigma} + \text{H.c.} \right) + U \sum_{i} n_{i\uparrow} n_{i\downarrow} + \sum_{\langle i,j\rangle} V_{i,j} n_{i} n_{j}$$

$$(1)$$

for the 2D system shown in Fig. 1. $\langle i, j \rangle$ denotes summation over all pairs of nearest neighbors, and spin $\sigma = \uparrow, \downarrow$. $c_{i,\sigma}^{\dagger}$ are electron creation operators, $n_i = \sum_{\sigma} c_{i,\sigma}^{\dagger} c_{i,\sigma}$ is the occupation-number operator, and U denotes the Coulomb repulsion between electrons on the same site. The hopping parameters t_{ij} , and intersite Coulomb interactions V_{ij} are defined in Fig. 1. Using second-order perturbation theory, one can transform Hamiltonian (1) into an effective t-J-V model

$$\mathcal{H} = -\sum_{\langle i,j\rangle,\sigma} t_{ij} \left(\hat{c}_{i,\sigma}^{\dagger} \hat{c}_{j,\sigma} + \text{h.c.} \right) +$$

$$+ \sum_{\langle i,j\rangle} J_{i,j} \left(\mathbf{S}_{i} \cdot \mathbf{S}_{j} - \frac{1}{4} n_{i} n_{j} \right) + \sum_{\langle i,j\rangle} V_{i,j} n_{i} n_{j}, \quad (2)$$

where $\hat{c}_{i,\sigma}^{\dagger} = c_{i,\sigma}^{\dagger} (1 - n_{i,-\sigma})$ are constrained electron creation operators, and \mathbf{S}_i denotes the spin- $\frac{1}{2}$ operator at site i. The exchange interactions between vanadium neighbors are parameterized as $J_{ij} = 4t_{ij}^2/U$.

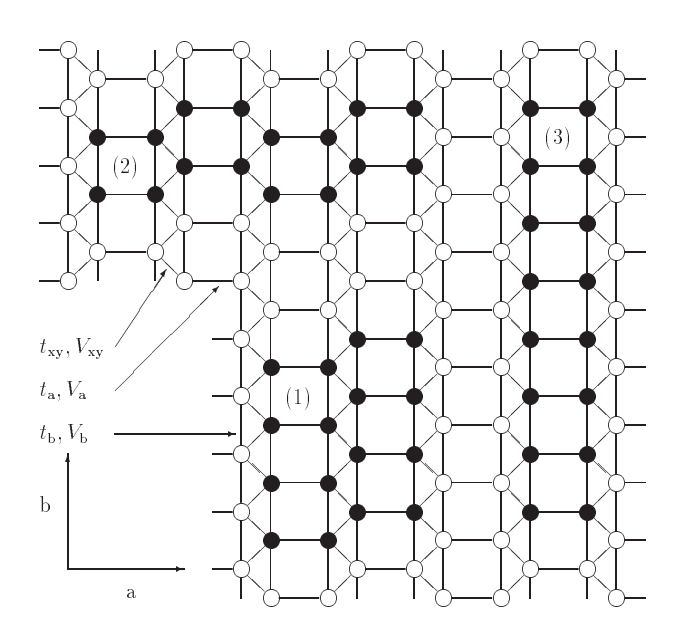


FIG. 1. Schematic structure of the (a,b) planes in NaV₂O₅ where the circles denote the vanadium sites. The black sites define clusters used in the calculation.

The loss function in EELS experiments is directly proportional to the dynamic density-density correlation function.²⁵ By including the long-range Coulomb interaction in the model within a random-phase approximation (RPA) one finds for the loss function

$$L(\omega, \mathbf{q}) = \operatorname{Im} \left[\frac{-1}{1 + v_{\mathbf{q}} \chi_{\rho}^{0}(\omega, \mathbf{q})} \right], \tag{3}$$

where

$$\chi_{\rho}^{0}(\omega, \mathbf{q}) = \frac{i}{\hbar} \int_{0}^{\infty} dt \, e^{i\omega t} \langle 0 | [\rho_{\mathbf{q}}(t), \rho_{-\mathbf{q}}] | 0 \rangle$$
 (4)

is the response function at zero temperature for the shortrange interaction models (1) and (2). χ_{ρ}^{0} depends on the energy loss ω and the momentum transfer \mathbf{q} . $|0\rangle$ is the ground state, $\rho_{\mathbf{q}}$ denotes the Fourier transform of n_i , and $v_{\bf q}=e^2N/(\epsilon_0\epsilon_{\rm r}v{\bf q}^2)$ is the long-range Coulomb interaction with unit cell volume v. N is the number of electrons per unit cell, and ϵ_o is the permittivity. The real part ϵ_r of the dielectric function can be obtained from the experiment. In the case of NaV₂O₅, one finds for momentum transfer in a direction $\epsilon_{\rm r}=7$, and in b direction $\epsilon_{\rm r}=5.^{22}$ The response function $\chi^0_{\rho}(\omega,\mathbf{q})$ and the optical conduction

tivity $\sigma_{\alpha}(\omega)$ are connected by the Kubo-Green relation

$$\sigma_{\alpha}(\omega) = \epsilon_0 \omega \lim_{\mathbf{q} \to 0} \operatorname{Im} \left[v_{\mathbf{q}} \chi_{\rho}^0(\omega, \mathbf{q}) \right], \qquad \mathbf{q} \parallel \alpha,$$
 (5)

where at zero temperature $\sigma_{\alpha}(\omega)$ is defined by

$$\sigma_{\alpha}(\omega) = \frac{1}{\omega} \operatorname{Re} \int_{0}^{\infty} dt \, e^{i\omega t} \langle 0 | j_{\alpha}(t) j_{\alpha} | 0 \rangle. \tag{6}$$

Here j_{α} with $\alpha = a, b$ are the components of the current operator parallel to a or b direction.

Equations (4), (6) for the response function and the optical conductivity are valid for zero temperature, whereas the experiments have been carried out at finite temperatures.²² However, for NaV_2O_5 one finds both experimentally^{22,26,27} and theoretically²⁹ that the spectra depend only weakly on temperature. Therefore, we may restrict ourselves to zero temperature. Equations (3) and (6) are evaluated by direct diagonalization using the standard Lanczos algorithm³⁰ which is limited to small clusters. For that reason, one can only observe localized excitations, and the calculation of the loss function (3) is limited to momentum transfers $\mathbf{q} \geq 2\pi/L$, where L is the cluster size in ${f q}$ direction.

III. LARGE OR SMALL INTERLADDER HOPPING

LDA band structure calculations⁶ and estimations based on empirical rules⁷ lead to similar values of the hopping amplitudes t_a , t_b perpendicular to and along the

ladders. However, there are significantly different estimations of the interladder hopping t_{xy} . A small value of $t_{xy}=0.012\mathrm{eV}$ is found in LDA calculations. Additional evidence for a small t_{xy} follows from the weak magnetic dispersion along the a-axis as observed by neutron scattering. No the other hand, a much larger value of $t_{xy}=0.3\mathrm{eV}$ was found from an estimation in Ref. 7. A relatively large interladder hopping of $t_{xy}=0.15\mathrm{eV}$ was also obtained from a comparison of calculated and experimental optical conductivity.

In Ref. 29, a finite temperature Lanczos method³¹ has been used to calculate the optical conductivity. The Lanczos approach is limited to small systems, and a cluster consisting of two ladders with four rungs [cluster (1) in Fig. 1] has been used in Ref. 29. However, when a calculation is restricted to finite systems, finite-size effects may distort the results. Finite-size effects affect delocalized excitations, which are important if the hopping parameters t_{ij} are large, and/or the momentum transfer \mathbf{q} is small. For that reason, the loss function $L(\omega, \mathbf{q})$ for small **q** is sensitive to finite-size effects. The calculation of the optical conductivity $\sigma_{\alpha}(\omega)$ is even more problematic, as it is obtained from $\chi_{\rho}^{0}(\omega, \mathbf{q})$ in the limit $\mathbf{q} \to 0$ [see Eq. (5)]. Since the importance of delocalized excitations can be decreased by increasing \mathbf{q} , we first study finite-size effects of the loss function $L(\omega, \mathbf{q})$ (Sec. IV). Already at finite \mathbf{q} we observe large effects even when a rather small value of the interladder hopping t_{xy} is used. This also means that the optical conductivity for the same cluster with a larger value of t_{xy} is even more affected by finite-size effects (see Sec. 6). Consequently, we can show that the results for the optical conductivity from Ref. 29 are not converged and cannot be used to support a large value of t_{xy} .

In the following, we shall use the hopping parameters $(t_a = 0.38\text{eV}, t_b = 0.17\text{eV}, t_{xy} = 0.012\text{eV})$ and the onsite Hubbard interaction (U = 2.8eV) from Ref. 6. Up to now the values of the intersite Coulomb interactions V_a , V_b and V_{xy} are not known exactly. Therefore we choose moderate values for V_a and V_b , so that the system is close to the quantum critical point caused by charge ordering. 20,21,29

IV. FINITE-SIZE EFFECTS

To investigate finite-size effects, one has to use clusters of different size. However, the cluster consisting of two ladders with four rungs [(1) in Fig. 1] is the largest to which the standard Lanczos algorithm can be applied at present. One way to overcome this problem is to enlarge the cluster in the direction of the momentum transfer, and to reduce it in perpendicular direction (so that the number of sites is kept constant). Of course, first one has to check that one does not distort the results by reducing the cluster perpendicular to the momentum transfer. To show this we use the effective t-J-V model

(2) with the above values of t_{ij} and U from Ref. 6. The intersite Coulomb interactions are chosen $V_a = 0.8 \text{eV}$, $V_b = 0.6 \,\mathrm{eV}$, and $V_{xy} = 0.9 \,\mathrm{eV}$. First we compare the loss function of the original cluster [indicated by (1) in Fig. 1, with periodic boundary conditions with those of two smaller clusters (not shown). The first consists of two ladders with two rungs for momentum transfer q parallel to a direction. The second cluster is an isolated ladder with four rungs for \mathbf{q} parallel to b direction. Note that periodic boundary conditions for these two smaller clusters make only sense in direction of the momentum transfer. Therefore we choose open boundary conditions perpendicular to the momentum transfer. Moreover, for the first of the two smaller clusters (momentum transfer in a direction) one has to use renormalized intersite Coulomb interactions $\bar{V}_a = V_a + V_b$ and $\bar{V}_b = 2V_b$. This follows from a straightforward analysis of the influence of adjacent rungs on the same ladder.

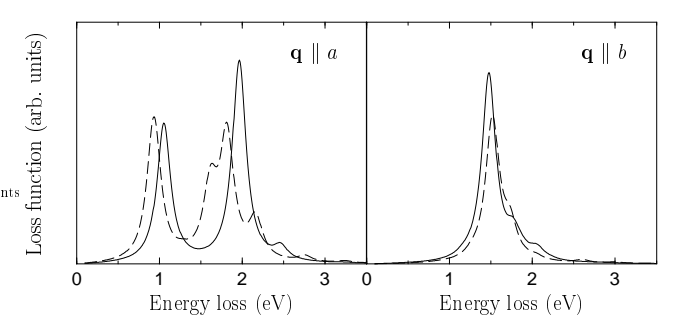


FIG. 2. Comparison of the loss function for two smaller clusters (full lines, see the text) and the system consisting of two ladders with four rungs [dashed lines, cluster (1) in Fig. 1]. We use the hopping parameters and the on-site Hubbard interaction of the t-J-V model from Ref. 6, the intersite Coulomb interactions are $V_a = 0.8 \mathrm{eV}$, $V_b = 0.6 \mathrm{eV}$, and $V_{xy} = 0.9 \mathrm{eV}$. The momentum transfer $\mathbf{q} = 0.3 \mathrm{Å}^{-1}$ is parallel to a direction (left panel) or b direction (right panel). The theoretical line spectra are broadened with Gaussian function of width $0.1 \mathrm{eV}$.

The results for the different clusters are shown in Fig. 2. The loss function for the original cluster (1) of Fig. 1 is drawn with dashed lines. The results for the smaller clusters with ${\bf q}$ in a or b direction are shown as solid lines in Fig. 2 (left or right panel, respectively). As can be seen from Fig. 2, apart from a small splitting of the second peak in the spectrum for ${\bf q}$ parallel to a direction there is good agreement between the results for the large cluster and both smaller systems. (Note that we use a small interladder hopping t_{xy} .)

Now we can study finite-size effects by increasing the two smaller clusters in the direction of momentum transfer. In this way we obtain clusters (2) and (3) in Fig. 1. In the left panel of Fig. 3 the loss function for cluster (2) with four ladders (and for the previous cluster with two ladders) are shown for different \mathbf{q} values in a direction. In the right panel of Fig. 3 we compare the ladder

systems with eight rungs [cluster (3) in Fig. 1] and with four rungs. One observes large finite-size effects for the loss function, especially for small momentum transfer **q**. Note that in particular, the larger clusters (2) and (3) from Fig. 1 (solid lines in Fig. 2) lead to additional peaks in the spectra. This clearly demonstrates that the original cluster (1) in Fig. 1, which is formed of two ladders with four rungs, is not large enough to allow reliable conclusions.

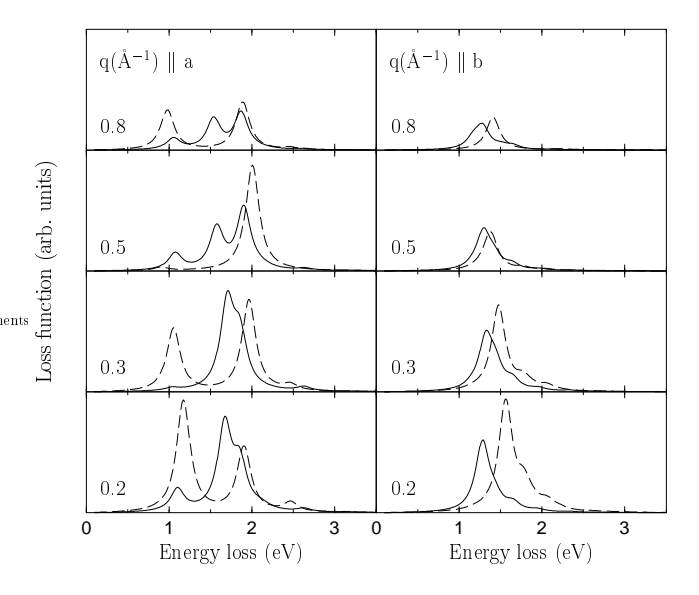


FIG. 3. Finite-size effects of the loss function for clusters with eight rungs (full lines) and four rungs (dashed lines); parameters as for Fig. 2.

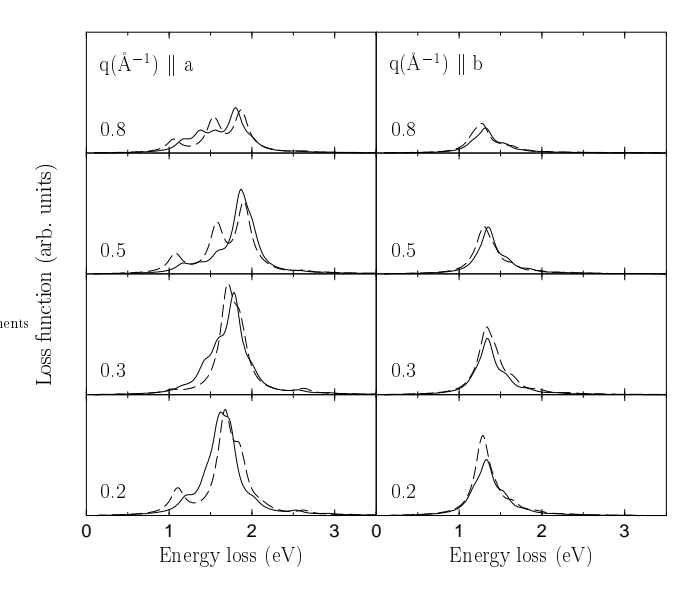


FIG. 4. Loss function for open boundary conditions (full lines) and periodic boundary conditions in \mathbf{q} direction (dashed lines); parameters as for Fig. 2.

To test if there are still finite size-effects for clusters (2) and (3), we next compare the spectra for closed and open boundary conditions in direction of momentum transfer. In the case of open boundary conditions one has to make sure that electrons on the edges of the cluster are still embedded in the local Coulomb potential that results from a zig-zag ordered state. For this purpose, sites on the edge of cluster (2) in Fig. 1 are assigned an additional on-site energy V_{xy} . Sites on the edges of cluster (3) that are not occupied in a zig-zag charge ordered state need an additional on-site energy V_b . As can be seen from Fig. 4 (left panel) there are only small differences between periodic (in q direction) and open boundary conditions for momentum transfer parallel to a direction, whereas one observes systematic discrepancies for small momentum transfer parallel to b direction [right panel of Fig. 4]. For $\mathbf{q} < 0.2 \text{Å}^{-1}$ there are large differences in both directions (not shown). We conclude that the convergence of the loss function is satisfactory for momentum transfer $\mathbf{q} \geq 0.2 \text{Å}^{-1}$. In the next section we use clusters (2) and (3) of Fig. 1 with periodic boundary conditions parallel to q direction for the calculation of the electron-energy loss spectrum.

V. ELECTRON-ENERGY LOSS SPECTRUM

For the comparison with the experimental loss function²² of NaV₂O₅ we use the full t-U-V model (1). The hopping parameters and on-site Hubbard interactions are taken from Ref. 6. The values of the intersite Coulomb interactions $V_a = 0.8 \, \text{eV}$, $V_b = 0.6 \, \text{eV}$ and $V_{xy} = 0.9 \, \text{eV}$ have been adjusted to obtain correct peak positions of the loss function.

In Fig. 5 the obtained loss function for the full model (1) is compared to the experimental spectra taken from Ref. 22. Very good agreement for the loss function with momentum transfer parallel to a direction [see panel (a) and (b) of Fig. 5] is found. In particular, the increasing width of the experimentally observed structure at 1-2eV with increasing **q** is reproduced. On the other hand, for momentum transfer parallel to b direction [panel (d) of Fig. 5] the observed structure at 1.0-1.7eV is not broad enough compared to the experiment [panel (c) of Fig. 5]. However, the agreement for momentum transfer parallel to b direction is significantly better for the full t-U-Vmodel (1) than for the t-J-V model (2).²² Note that for momentum transfer in a direction the results for both models differ only slightly. This implies that there are different basic mechanisms for excitations with momentum transfer in a or b direction: doubly occupied sites are only important for momentum transfer parallel to bdirection.

Now let us discuss the character of these excitations in more detail. In the ground state all rungs of the ladders are found to be essentially singly occupied. Since the system is close to the charge order transition, ^{20,29}

one can illustrate the nature of the excitations using a zig-zag ordered ground state.

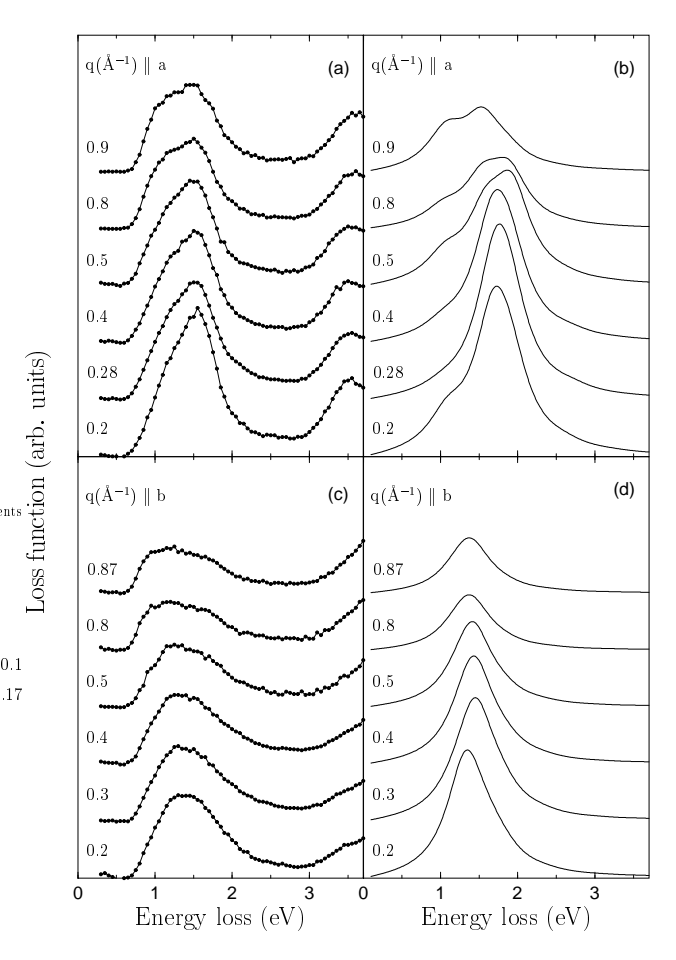


FIG. 5. Comparison of experimental data for $\rm NaV_2O_5$ (left), taken from Ref. 22, and the calculated loss function plotted with an energy resolution of 0.3eV (right). The hopping parameters and the on-site Hubbard interaction of the t-U-V model are used from Ref. 6, the intersite Coulomb interactions are $V_a = 0.8 \, \rm eV$, $V_b = 0.6 \, \rm eV$, and $V_{xy} = 0.9 \, \rm eV$.

Disturbance of the charge ordering by electron hopping on a rung [process (a1) in Fig. 6] is found to be the basic mechanism for excitations with momentum transfer parallel to a direction. The excitation energy is dominated by V_b , and other rungs of the ladders are only involved via V_b and V_{xy} . Note that process (a1) can also be interpreted as a transition from a bonding to an antibonding state of a singly occupied rung.³³ In addition to this one electron transition, there are also collective transitions that involve two [process (a1)+(a2) in Fig. 6] or three [process (a1)+(a2)+(a3) in Fig. 6] adjacent rungs on different ladders. The collective nature of these transitions results from the interladder Coulomb interaction V_{xy} . The role of V_{xy} can best be illustrated in the limit of small electron hopping (see Fig. 6). In this case the excitation energies are $2V_b$, $(4V_b - V_{xy})$, and $(6V_b - 2V_{xy})$

for the processes (a1), (a1)+(a2), and (a1)+(a2)+(a3).

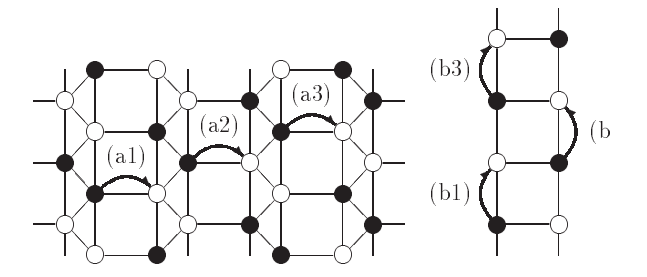


FIG. 6. Illustration of the basic excitations with momentum transfer parallel to a direction (left) and b direction (right). In addition to the local transition on one rung [process (a1)], for momentum transfer parallel to a direction one also observes collective transitions of two or three adjacent rungs on different ladders coupled by the interladder Coulomb interaction V_{xy} [process (a1)+(a2) or (a1)+(a2)+(a3)]. The creation of one unoccupied and one doubly occupied rung [process (b1)] is the basic mechanism for excitations with momentum transfer parallel to b direction. Electron movement can lead to an increased distance between unoccupied and doubly occupied rung [processes (b1)+(b2), (b1)+(b2)+(b3)].

The theoretical spectra for momentum transfer parallel to a direction [see panel (b) of Fig. 5] mainly consist of three excitations at 1.2eV, 1.6eV, and 1.8eV that contribute to the structure at 1-2eV energy loss. With increasing momentum transfer ${\bf q}$ spectral weight shifts from the excitation at 1.6eV to the one at 1.8eV. The three excitations differ in the contribution of processes shown in Fig. 6. The excitation at 1.2eV is rather delocalized and consists mainly of multi-electron transitions [processes (a1)+(a2) or (a1)+(a2)+(a3) in Fig. 6]. The other peaks result from more localized processes that are dominated by one electron transitions [process (a1) in Fig. 6]. In addition, the transition (a1)+(a2) in Fig. 6 contributes to the excitation with energy loss 1.6eV.

The excitations that correspond to the structure at 1.0-1.7eV for momentum transfer parallel to b direction [see panel (d) of Fig. 5] can be interpreted as transitions to states with one unoccupied and one doubly occupied rung [process (b1) in Fig. 6]. The excitations differ in the distance between unoccupied and doubly occupied rung, see processes (b1)+(b2) and (b1)+(b2)+(b3). These excitations are not influenced by the interladder Coulomb interaction V_{xy} , since the contribution of the V_{xy} part of Hamiltonian (1) is not changed by electron movement in one ladder of the zig-zag ordered system at quarter filling, and an unoccupied or a doubly occupied rung can be easily moved along the ladder. Since we can only observe rather localized excitations by direct diagonalization of small clusters there is a lack of spectral weight in our theoretical spectra [panel (d) of Fig. 5] compared to the experimental data [panel (c) of Fig. 5].

VI. OPTICAL CONDUCTIVITY

Before we discuss our results for the optical conductivity, we briefly study their finite-size effects. A good agreement between calculated and experimental optical conductivity was obtained from a finite temperature Lanczos method.²⁹ In Ref. 29 cluster (1) in Fig. 1 with periodic boundary conditions was used, and the parameters of the t-J-V model (2) were chosen as $t_a = 0.4 \text{eV}$, $t_b=0.2{\rm eV},\,t_{xy}=0.15{\rm eV},\,U=4{\rm eV},\,V_a=V_b=0.8{\rm eV},$ and $V_{xy}=0.9{\rm eV}.$ However, for this system we obtain large finite-size effects as can be seen from a comparison of the results for periodic [full lines in panel (a) and (b) of Fig. 7] and open boundary conditions [dashed lines in panel (a) and (b) of Fig. 7. Consequently, the cluster formed of two ladders with four rungs is not large enough to obtain reliable results for the optical conductivity. To overcome this problem we again use clusters (2) and (3) of Fig. 1 for the calculation of σ_a and σ_b . (In Sec. IV we have shown that a reduction of the cluster perpendicular to the momentum transfer affects the loss function only weakly if the interladder hopping t_{xy} is small. This statement remains valid for the calculation of the optical conductivity if the direction of the momentum transfer is replaced by the direction of the electric field.)

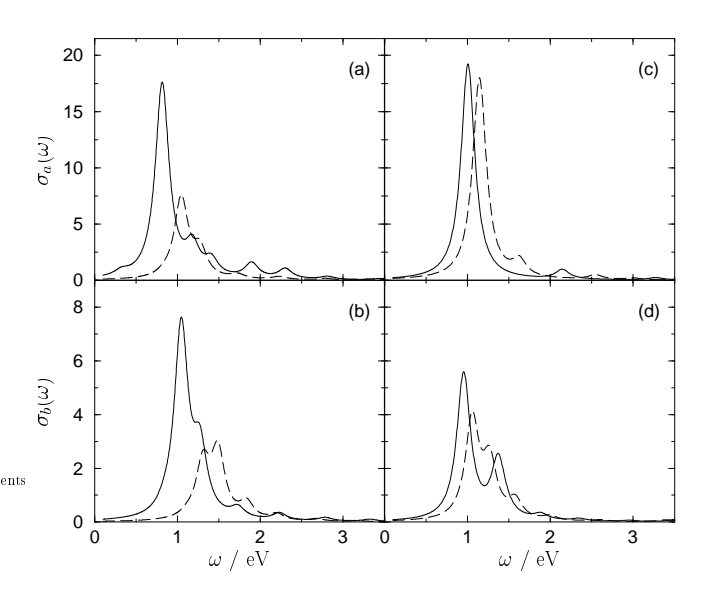


FIG. 7. Optical conductivity of cluster (1) in Fig. 1 [panels (a) and (b), parameters of the t-J-V model are used from Ref. 29], cluster (2) and (3) [panels (c) and (d), parameters of the t-U-V model as for Fig. 5] plotted with an energy resolution of 0.1eV for periodic boundary conditions (full lines) and open boundary conditions (dashed lines).

For the comparison with the experimental optical conductivity³² of NaV₂O₅ we use the full t-U-V model (1), and the same parameters as for the calculation of the loss function in Sec. V. In panels (c) and (d) of Fig. 7 the results for σ_a and σ_b using clusters (2) and (3) of Fig. 1

are shown. As a result of finite-size effects discussed in Sec. IV we obtain only a qualitative agreement of the calculated optical conductivity and the experimental data of Ref. 32. In analogy to the loss function, there is a lack of spectral weight for σ_b , and the ratio $r = I_a/I_b = 3.3$ of total a and b intensities is larger than the experimental value of 2.2. Note, however, that the differences of the optical conductivity for periodic (full lines) and open boundary conditions (dashed lines) using clusters (2) and (3) of Fig. 1 are much smaller than the differences for the cluster (1). In contrast to Ref. 29 we have used a small interladder hopping t_{xy} to describe the optical conductivity. Consequently, we conclude from the comparison with the experiment that interladder hopping is of minor importance for a realistic description of charge excitations in NaV₂O₅. The same was found in a previous theoretical study²³ of the optical conductivity where a t-J-Vmodel was investigated which was slightly modified by an additional symmetry-breaking on-site energy.

VII. CONCLUSIONS

Summing up, we have calculated the EELS spectrum and the optical conductivity for the quarter-filled ladder compound α' -NaV₂O₅ by exact diagonalization of small systems using the standard Lanczos algorithm. Our analysis shows that finite-size effects for these calculations are very important, in particular for the loss function with small momentum transfer and for the optical conductivity. We minimize these finite-size effects by using clusters of different shape depending on the direction of momentum transfer and the direction of the electric field respectively. The results for the loss function are in good agreement with experimental spectra. We also obtain a qualitative description of the optical conductivity. The comparison with the experiment confirms that a large value of the interladder hopping is not needed for a realistic description of charge excitations in NaV₂O₅. We find that the basic mechanism for excitations strongly depends on the direction of momentum transfer. For momentum transfer parallel to a direction three different excitations are observed. They differ in their degree of delocalization. The collective character of the delocalized processes results from the interladder Coulomb interaction. The excitations for momentum transfer parallel b direction can be characterized by the creation of an unoccupied and a doubly occupied rung.

ACKNOWLEDGEMENTS

Discussions with S. Atzkern, J. Fink, M. S. Golden, R. E. Hetzel, J. Richter, and M. Vojta are gratefully acknowledged. This work was supported by DFG through the research program of the GK 85, Dresden. The calculations were performed on the Origin 2000 at Technische

- ¹ M. Weiden, R. Hauptmann, C. Geibel, F. Steglich, M. Fischer, P. Lemmens, and G. Güntherodt, Z. Phys. B **103**, 1 (1997).
- ² M. Isobe and Y. Ueda, J. Phys. Soc. Jpn. **65**, 1178 (1996).
- ³ Y. Fujii, H. Nakao, T. Yoshihama, M. Nishi, K. Nakajima, K. Kakurai, M. Isobe, Y. Ueda, and H. Sawa, J. Phys. Soc. Jpn. **66**, 326 (1997).
- ⁴ A. Capry and J. Galy, Acta Cryst. **31**, 1481 (1975).
- ⁵ H. G. Schering, Y. Grin, M. Kaupp, M. Sommer, R. K. Kremer, O. Jepsen, T. Chatterji, and M. Weiden, Z. Kristallogr. **213**, 246 (1998).
- ⁶ H. Smolinski, C. Gros, W. Weber, U. Peuchert, G. Roth, M. Weiden, and C. Geibel, Phys. Rev. Lett. 80, 5164 (1998).
- ⁷ P. Horsch and F. Mack, Eur. Phys. J. B **5**, 367 (1998).
- ⁸ M. Köppen, D. Pankert, R. Hauptmann, M. Lang, M. Weiden, C. Geibel, and F. Steglich, Phys. Rev. B 57, 8466 (1998).
- T. Ohama, H. Yasuoka, M. Isobe, and Y. Ueda, Phys. Rev. B 59, 3299 (1999).
- ¹⁰ H. Seo and H. Fukuyama, J. Phys. Soc. Jpn. **67**, 2602 (1998).
- ¹¹ M. V. Mostovoy and D. I. Khomskii, Solid State Commun. 113, 159 (2000).
- ¹² P. Thalmeier and P. Fulde, Europhys. Lett. **44**, 242 (1998).
- ¹³ Y. Fagot-Revurat, M. Mehring, and R. K. Kremer, Phys. Rev. Lett. **84**, 4176 (2000).
- ¹⁴ J. Lüdecke, A. Jobst, S. van Smaalen, E. Morré, C. Geibel, and H.-G. Krane, Phys. Rev. Lett. 82, 3633 (1999).
- ¹⁵ S. van Smaalen and J. Lüdecke, Europhys. Lett. 49, 250 (2000).
- ¹⁶ J. L. deBoer, A. Meetsma, J. Baas, and T. T. M. Palstra,

- Phys. Rev. Lett. 84, 3962 (2000).
- ¹⁷ T. Ohama, A. Goto, T. Shimizu, E. Ninomiya, H. Sawa, M. Isobe, and Y. Ueda, preprint (cond-mat/0003141).
- ¹⁸ A. Bernert, T. Chatterji, P. Thalmeier, and P. Fulde, preprint (cond-mat/0012327).
- ¹⁹ P. Fulde, Ann. Physik **6**, 178 (1997).
- ²⁰ M. Vojta, R. E. Hetzel, and R. M. Noack, Phys. Rev. B 60, R8417 (1999).
- ²¹ M. Vojta, A. Hübsch, and R. M. Noack, Phys. Rev. B 63, 045105 (2001).
- ²² S. Atzkern, M. Knupfer, M. S. Golden, J. Fink, A. N. Yaresko, V. N. Antonov, A. Hübsch, C. Waidacher, K. W. Becker, W. von der Linden, G. Obermeier, and S. Horn, Phys. Rev. B 63, 165113 (2001).
- ²³ S. Nishimoto and Y. Ohta, J. Phys. Soc. Jpn. **67**, 3679 (1998).
- ²⁴ S. Nishimoto and Y. Ohta, J. Phys. Soc. Jpn. **67**, 4010 (1998).
- ²⁵ S. E. Schnatterly, Solid State Phys. **34**, 275 (1977).
- ²⁶ V. C. Long, Z. Zhu, J. L. Musfeldt, X. Wei, H.-J. Koo, M.-H. Whangbo, J. Jegoudez, and A. Revcolevshi, Phys. Rev. B 60, 15721 (1999).
- ²⁷ C. Presura, D. van der Marel, A. Damascelli, and R. K. Kremer, Phys. Rev. B 61, 15762 (2000).
- ²⁸ T. Yosihama, M. Nishi, K. Nakajima, K. Kakurai, Y. Fuji, M. Isobe, C. Kagami, and Y. Ueda, J. Phys. Soc. Jpn. 67, 744 (1998).
- ²⁹ M. Cuoco, P. Horsch, and F. Mack, Phys. Rev. B **60**, R8438 (1999).
- ³⁰ For example, see H. Q. Lin and J. E. Gubernatis, Computers in Physics **7**, 400 (1993), and references therein.
- 31 J. Jaklič and P. Prelovšek, Phys. Rev. B $\mathbf{49},\,5065$ (1994).
- ³² A. Damascelli, D. van der Marel, M. Grüninger, C. Presura, T. T. M. Palstra, J. Jegoudez, and A. Revcolevschi, Phys. Rev. Lett. 81, 918 (1998).
- ³³ A. Damascelli, C. Presura, D. van der Marel, J. Jegoudez, and A. Revcolevschi, Phys. Rev. B 61, 2535 (2000).